THE ASTROPHYSICAL JOURNAL, 428:370–376, 1994 June 10

THE MID-INFRARED SPECTROMETER ON THE INFRARED TELESCOPE IN SPACE (IRTS) MISSION

THOMAS L. ROELLIG
MS 245-6, NASA Ames Research Center, Moffett Field, CA 94035-1000
TAKASHI ONAKA
Department of Astronomy, School of Science (Formerly Faculty of Science), University of Tokyo, Bunkyo-ku Tokyo 113, Japan
THOMAS J. MCMAHON
Yerkes Observatory, P.O. Box 258, Williams Bay, WI 53191
AND
T. TANABÉ
Institute of Astronomy, Faculty of Science, University of Tokyo, Mitaka, Tokyo 181, Japan
Received 1993 February 19; accepted 1993 December 10

ABSTRACT

The Mid-Infrared Spectrometer (MIRS) is one of the four focal plane instruments on the Infrared Telescope in Space (IRTS) mission. The instrument has been constructed, tested, and calibrated in the laboratory and is presently scheduled to be launched by a Japanese expendable launch vehicle as part of the Space Flyer Unit-1 mission in early 1995. The wavelength coverage of the MIRS ranges from 4.5 to 11.7 μm, with a spectral resolution of 0.23 to 0.36 μm. With the cryogenically cooled optics of the IRTS telescope assembly, the MIRS will be able to make an extremely sensitive survey of both point-source and extended objects over an estimated 10% of the sky.

Subject headings: artificial satellites, space probes — infrared: general — instrumentation: spectrographs

1. INTRODUCTION

The Infrared Telescope in Space (IRTS) is one of seven experiments on the first Space Flyer Unit (SFU-1), scheduled for launch from Tanegashima Space Center in Japan in early 1995. After a planned mission duration of 6–18 months, the SFU-1 will be retrieved by NASA's Space Transportation System and returned to Earth for refurbishment and reuse. The IRTS telescope is cooled by superfluid helium, lowering the infrared background seen by the instruments to the levels set by the natural Zodiacal, Galactic, and cosmological emission. Four scientific instruments and a near-infrared star sensor used for telescope pointing reconstruction share a common focal plane in the IRTS telescope. This paper describes one of the instruments, the Mid-Infrared Spectrometer (MIRS). Descriptions of the other three instruments and the telescope facility can be found elsewhere (Murakami et al. 1994; Onaka et al. 1993; Bock et al. 1993; Noda et al. 1994; Shibai et al. 1994; Lange et al. 1994). A brief review of the telescope and mission parameters is given in § 2, the MIRS design and description is given in § 3, the results of the laboratory calibrations are given in § 4, and an estimate of the on-orbit sensitivity of the MIRS and its ability to meet its science goals is given in § 5.

2. THE IRTS MISSION

After separation from the launch booster, the SFU will be inserted into a nearly circular, 482 km altitude, 28°.5 inclination orbit. After a checkout period lasting approximately one week, the IRTS aperture cover will be ejected and observations will begin from all four focal plane instruments for a period of 20 days. Upon termination of the 20 day IRTS observation period, the IRTS will be turned off and other experiments on the SFU-1 will commence. Present tests of the flight cryostat indicate that the superfluid helium hold time will be approximately 35 days, more than adequate to last through the observation period. After a period of 6–18 months from launch, the SFU-1 is scheduled to be retrieved by NASA's Space Transportation System for refurbishment and reuse in the future.

The IRTS will orbit the Earth with the telescope sweeping across the sky at a rate of 0°.067 $\sec^{-1}$ in great circles that are defined by the various Earth and Sun avoidance angle constraints (Murakami et al. 1994). Each of the great circle scans will be offset from one another by approximately 0°.067, or approximately one-half of the MIRS beam size. This means that the IRTS will survey up to approximately 1.3 steradians or 10% of the sky during the anticipated 20 days of IRTS observations.

3. THE MIRS INSTRUMENT DESCRIPTION

The modest scale of the IRTS mission presented all of the focal plane instruments with severe size, weight, power dissipation, and data rate constraints. As the IRTS facility did not provide infrared calibration sources, each instrument had to incorporate its own. To meet the MIRS science goals, a low resolution spectrometer operating from 5 to 11 μm was indicated. In order to meet the power and weight constraints it was decided that the MIRS would have a fixed grating with a cold instrument entrance aperture shutter as the only moving part. Closing this shutter provides an absolute zero infrared background condition for measuring detector dark currents and also blocks the emission of stray infrared light from the MIRS when the internal calibration source is on. If this stray light were not blocked, it could produce optical interference in the other focal plane instruments during calibration periods. Since all of the IRTS focal plane instruments will be operated simultaneously, it was important that all sources of optical, electrical, thermal, and mechanical interference between the

instruments be eliminated. The MIRS optical design that was developed to meet the above constraints is shown in Figure 1. The overall specifications are given in Table 1. Further details of the individual MIRS components are given below.

3.1. *Optical Components*

The IRTS telescope output is divided among the four focal plane instruments and the near-IR star sensor by a set of pick-off mirrors mounted just in front of the telescope focal plane. The MIRS pick-off mirror is constructed of TiN-coated polished aluminum and was manufactured by Nikon Corporation of Japan. The IRTS telescope images the sky off of this mirror onto the 1.4 × 1.4 mm (8′ × 8′ field of view) MIRS entrance aperture. A 3.4 μm long-pass filter located immediately behind the entrance aperture is used to eliminate second-order dispersed light from the grating at wavelengths shorter than 6.8 μm. As this filter also begins to gradually cut out light at wavelengths longer than 8 μm, it also limits the infrared emis-

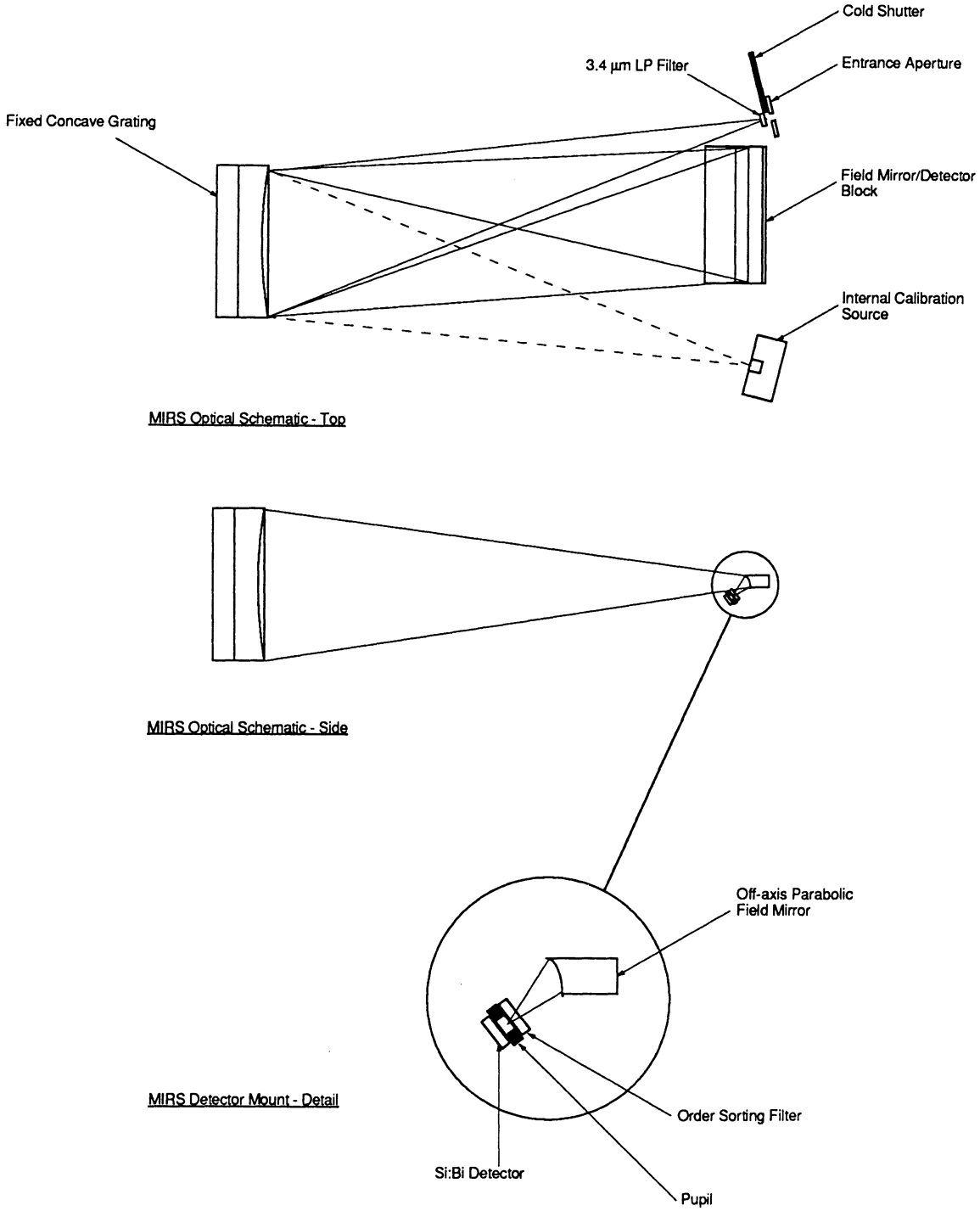

FIG. 1.—Schematic diagram of the optical layout of the Mid-Infrared Spectrometer

TABLE 1

MIRS SPECIFICATIONS

Parameter	Value
Wavelength range (μm)	4.495–11.703
Resolution (μm)	0.23–0.36
Size (mm)	Irregular shape—210 × 137 × 75 overall
Weight (g)	805
Electrical power dissipation	
Cold electronics (mW)	4
Warm electronics (W)	2.9
Operating temperature	1.8 K
Detectors	32 Si:Bi photoconductors, Aerojet Electro Systems
Entrance Aperture (mm)	1.4 × 1.4 (0°.14 × 0°.14 on sky)
Integrating Amplifiers	Model JF-4, IR Labs
Cold Multiplexers	CD4067B, RCA Electronics Corp.
Warm electronics package	Hamamatsu Photonics K. K.
MIRS data rate (bits s^{-1})	1188 (standard operating mode) 594 (reduced data-rate mode)

sion that could conceivably arise from the warm JFETs within the MIRS and interfere with the longer wavelength instruments on the IRTS. The light emerging through the entrance long-filter then travels the length of the MIRS and strikes a concave grating which simultaneously refocuses the light onto the field mirror set and disperses it.

The MIRS grating is of a novel design that incorporates variable line spacings and blaze angles in order to both correct for astigmatism and flatten the focal plane (Harada & Kita 1980). With this grating design, essentially all of the aberrations can be eliminated at a given wavelength by adjusting the groove spacing parameters. In our application, we need to cover a wide range of wavelengths, so the grating parameters given in Table 2 were chosen to give the best compromise performance over the entire wavelength range (Onaka 1994). As a result, there are some uncorrected aberrations (mostly astigmatism) remaining for the wavelengths on each side of the 6 μm aberration minimum. The effect of this aberration is to broaden the base of the spectral response function for a single detector, but to leave the full width at half-maximum (FWHM) value at the level set by the dimensions of the entrance aperture and detector. In the worst case, the increase in the wings of the response function will be 0.15 μm, which is still less than the 0.23 μm resolution imposed by the size of the MIRS entrance aperture and detector. With the MIRS grating there are essentially no aberrations in the spatial dimension, so that the spatial resolution of extended sources is not compromised.

TABLE 2

MIRS GRATING PARAMETERS

Parameter	Value
Grating size (mm)	50 × 50 × 17
Effective area illuminated by telescope (mm)	46 dia
Grating surface	Gold
Radius of curvature (mm)	160
Incidence angle	14°
Blaze wavelength (μm)	6.0
Nominal grating spacing (mm^{-1})	37.56
Spacing variation parameters[a]	
b2	0.12822
b3	0.026531
b4	0.0076868

[a] Definitions can be found in Harada & Kita 1980 or Onaka 1994.

Further details of the MIRS grating construction and performance can be found in Onaka (1994).

The spectrally dispersed image of the MIRS entrance aperture is focused by this grating onto 32 off-axis parabolic field mirrors. These field mirrors in turn image the grating onto 0.85 mm diameter pupils located immediately in front of the MIRS infrared detectors. Between the field mirrors and the pupils, 6.1 μm long-pass interference filters are used for removing second-order light in the 24 longest wavelength channels. In order to keep the optical path length the same for all the channels, wide-band anti-reflection coated germanium of the same thickness as the long-pass order-sorting filters is located in front of the eight shortest wavelength channels. The entire inside of the MIRS is highly baffled and is painted with an infrared-absorbing black paint to minimize stray light.

3.2. *Detectors*

The MIRS uses 32 individual Si:Bi photoconductor detectors to detect incoming infrared radiation. Detectors of this construction were chosen because of their relative freedom, when biased appropriately, from long-term time-constant effects in low background environments and their relative immunity to radiation-induced responsivity changes (Young 1989). Measurements taken in the laboratory indicate that the detector responsivity change is expected to be less than 5% after a passage through the South Atlantic Anomaly. The measured performance of the MIRS flight detectors is given in Table 3.

3.3. *Electronics*

A schematic diagram of the cold electronics is shown in Figure 2. The integrating amplifiers were obtained commercially (Infrared Laboratories, Model JF-4) and include internal heaters to prevent carrier freeze-out in their JFET transitors at liquid helium temperatures. A total heater power of 3.0 mW for all 32 units is sufficient to warm the amplifiers enough to meet the MIRS performance specifications of an output impedance of less than 50 k ohm and a voltage gain of better than 0.9. With the 1.0 mW of bias power that the integrating amplifiers dissipate when operational, a total of 4.0 mW of electrical power is generated in the cold electronics that needs to be absorbed by the superfluid helium cryogen. The other active cold electronics components, the CMOS cold multiplexers, dissipate negligible power at the low switching rates of the MIRS. Each of the amplifiers is enclosed in its own

TABLE 3

MIRS DETECTOR CHARACTERISTICS

Parameter	Value
Detector material	Si:Bi
Supplier	Aerojet ElectroSystems
Size (mm)	1.1 × 1.6 × 0.5
Bias voltage (V)	2.0
Average measured dark current at 2.0 V bias and 1.8 K operating temperature ($e^{-} s^{-1}$)	<1400
Quantum efficiency[a]	6%–70% (27% average)
Photoconductive gain-quantum efficiency product[b]	0.03–0.28
Responsivity[b] ($A W^{-1}$)	0.1–2.6

[a] Measured by vendor at 3.0 V bias, 2.8 K operating temperature, and 13.4 μm wavelength.

[b] Measured at 2.0 V bias, 1.8 K operating temperature.

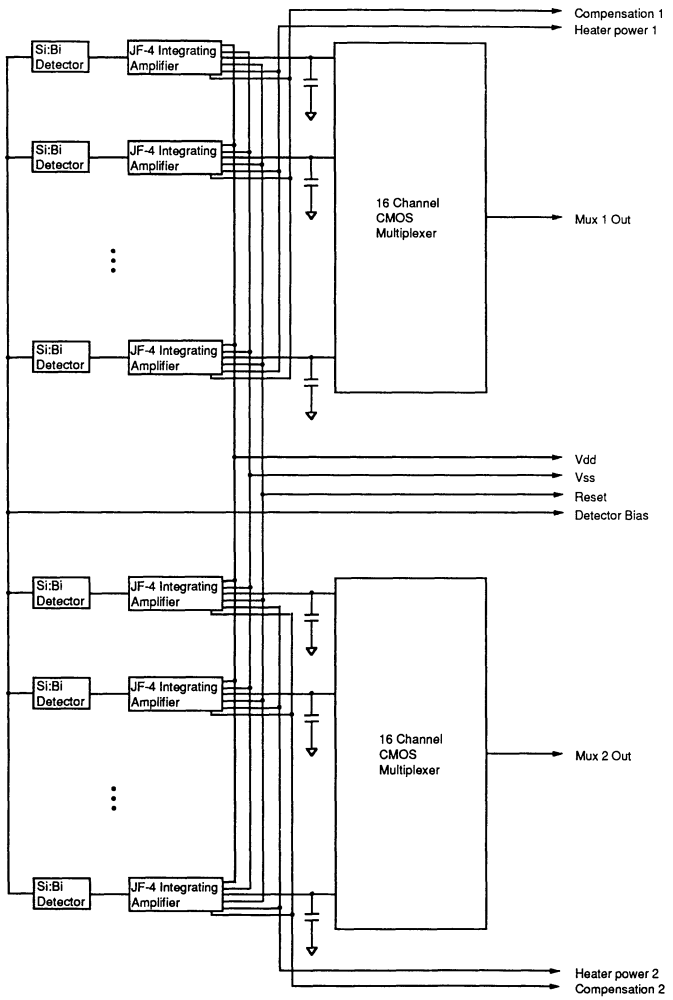

FIG. 2.—Schematic diagram of the 1.8 K electronics in the Mid-Infrared Spectrometer.

individual light-tight radiation shield, so that the warm JFETs do not introduce any extra infrared background onto the detectors. The input capacitance of the integrating amplifiers is 7.5 pF, which means that the output of the amplifiers is approximately 1.2×10^{11} V s^{-1} amp^{-1}. Each of the two cold multiplexers consists of a 16 channel commercial CMOS-type unit (RCA Corp., CD 4067B). In order to keep the multiplexer on-state impedance low throughout the output voltage range of the integrating amplifiers, the multiplexers are biased with ± 5 volts and are also addressed with ± 5 V logic.

The warm electronics package for the MIRS was constructed by Hamamatsu Photonics K. K. of Japan and is diagrammed schematically in Figure 3. The final output of the electronics is a serial data stream of 16 bit numbers from the detectors, thermometers, and voltage references. The total noise of the detector/electronics system with the bias voltage applied to the detector, no incident infrared flux, and sampling each detector at a 2 Hz rate, was measured to be 180 electrons read^{-1}, referred to the detector.

During most of the IRTS mission, the integrated signal from each MIRS detector output will be sampled at a rate of 2 Hz, allowing four samples in the time it takes a point-source object to cross the MIRS entrance aperture. For approximately one-third of the mission orbits, the SFU-1 spacecraft will not pass over the field of view of a Deep Space Network receiving station. In these orbits, the recorded data would overflow the onboard memory if the data rate from the instruments were not reduced. As a result, in the case of these orbits, the IRTS will enter a reduced data-rate operations mode where the MIRS detector outputs are sampled at a rate of 1 Hz.

3.4. *In-Flight Calibration Source and Thermometry*

In addition to calibrations provided by observing standard astronomical sources while scanning the sky, the MIRS will be calibrated every 15 minutes on-orbit by an internal calibration source. Each of these calibration periods will last one minute, during which all of the focal plane instruments on the IRTS will conduct their internal calibrations. The MIRS calibration source consists of a hot metal wire with a tiny drop of black epoxy acting as a blackbody emitter. Tests have shown that the wire/epoxy combination heats up reproducibility to a constant emission level in approximately 3 seconds. The entire wire and epoxy bead assembly is located in an enclosure with a 12.5 μm diameter aperture hole, which defines a point source and also limits the amount of far-infrared radiation from the MIRS calibration source that might interfere with the other longer-wavelength IRTS focal plane instruments. As is shown in Figure 1, the calibration source is located at the same angle relative to the grating as is the entrance aperture, but on the other side of the grating. As a result, the wavelength assignments for each detector are reversed compared to the wavelength assignments for the light from the MIRS entrance aperture. Some of the long-pass order-sorting filters are therefore in the wrong positions with this scheme, so that little infrared flux is seen in the eight longest-wavelength detectors. In spite of these disadvantages, tests have shown that the calibration source will reproducibly illuminate all of the 24 shortest wavelength detectors so that gain and detector responsivity variations can be monitored. Two Si diode thermometers (Lakeshore Cryotronics, Model DT-470) are used to monitor the temperature of the MIRS. One of the thermometers is mounted on the base of the MIRS housing, the second is mounted on the MIRS detector block holding the Si:Bi detectors.

4. LABORATORY CALIBRATIONS

The MIRS was tested and calibrated extensively in the laboratory both at NASA/Ames and the Institute for Space and Astronautical Science (ISAS) prior to delivery to the spacecraft. For the initial tests and calibration the instrument was mounted at the focal plane of the IRTS flight telescope and both telescope and instrument were enclosed in a special test cryostat located at ISAS. In order to emulate the low infrared background conditions expected on-orbit, a combination of cold neutral density filters were used, reducing the infrared background seen by the MIRS/IRTS telescope in the laboratory to that of a 295 K gray body with an emissivity of $(5.6 \pm 1.5) \times 10^{-8}$. Laboratory measurements of the ND filters using an infrared spectrometer showed their spectral response to be flat to within 5% over the wavelength range of the MIRS. Using this test cryostat, together with calibrated blackbody sources, the MIRS sensitivity, telescope focus, spectral range and resolution, polarization, and detector time-constant effects were measured in the laboratory. The results from these calibrations are presented in more detail below. After these calibrations were performed, the telescope assembly was installed

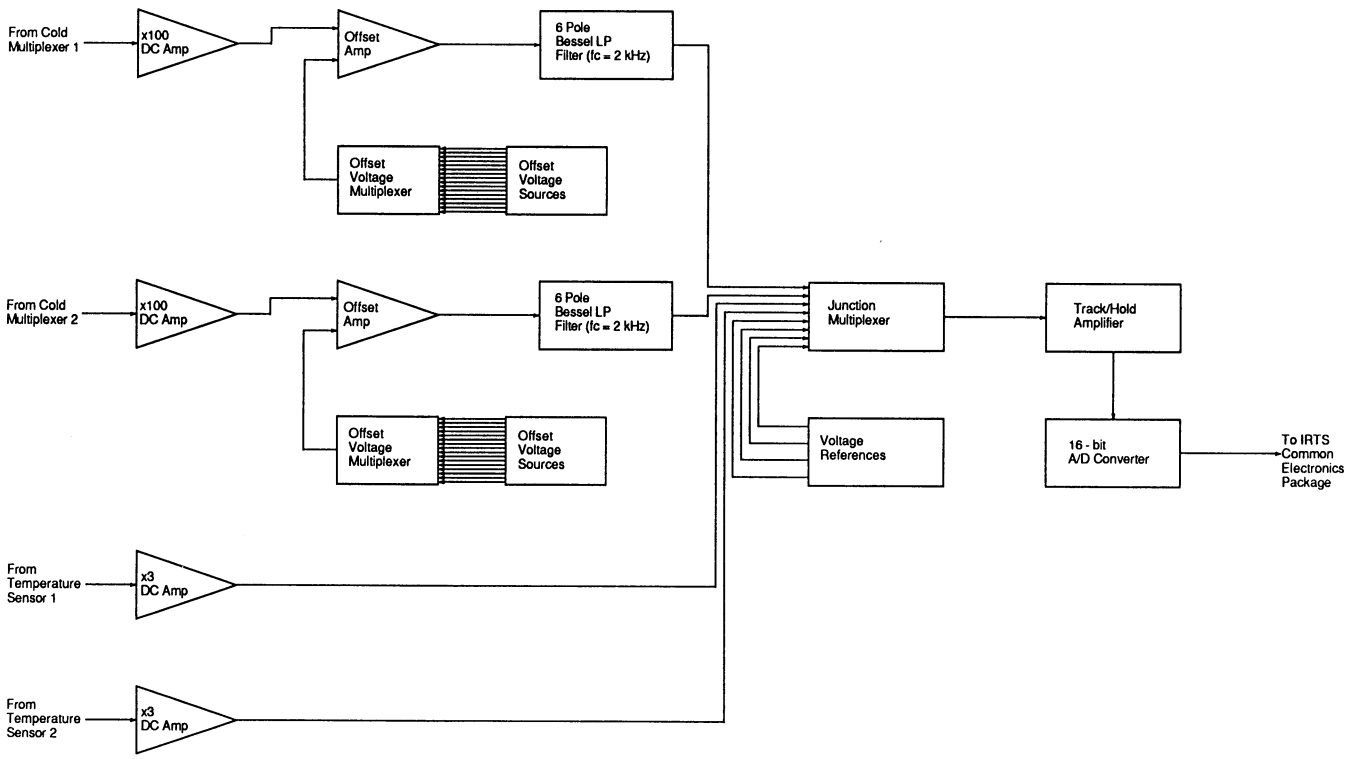

FIG. 3.—Schematic diagram of the warm electronics for the Mid-Infrared Spectrometer

in the IRTS flight cryostat together with the other focal plane instruments, and tests were conducted ensuring that there was no significant cross talk or interference between any of the instruments while they were all operational.

Spectral and tests of the MIRS were made with a calibrated circular variable filter, a series of calibrated narrow bandpass filters, and two polymer plastic filters whose absorption spectrum had been previously been determined at NASA/Ames with a Fourier transform spectrometer. The full wavelength coverage of the MIRS was found to range from 4.495 to 11.703 μm, while the center wavelengths for the detectors ranged from 4.608 to 11.590 μm. The relationship between the detector center wavelength and the detector spatial position was almost exactly linear. In theory, the grating and optical parameters of the MIRS should give a spectral resolution with a FWHM of 0.23 ± 0.01 μm over the full spectral range of the MIRS (Onaka 1994). In actuality, once corrected for the finite spectral width of the test filters, the measured instrumental FWHM spectral resolution was found to range from a minimum of 0.23 μm at a wavelength of 6.7 μm to a maximum of 0.36 μm at 10.8 μm. The reason for the observed excess in the spectral bandwidth at the longer wavelengths is unknown at this time, although since our test set-up did not fully illuminate the grating, our measurements are only approximations to the true spectral resolution that will be achieved on-orbit. The on-orbit spectral resolution will be determined by careful comparison of observations of standard astronomical sources with known spectral lines.

The MIRS instrumental polarization was measured using a wire grid polarizer. Significant instrumental linear polarization was observed in the MIRS, with the angle of polarization coincident with the grating dispersion direction. The magnitude of the instrumental polarization is shown in Figure 4, and was found to increase with wavelength, from a value of nearly zero at the shortest wavelengths up to a value of approximately 30% at 11.6 μm. This observed instrumental polarization is unfortunate, because although few of the MIRS astronomical sources are anticipated to be highly polarized in the mid-infrared, the instrumental polarization will add to the flux measurement uncertainties for those objects for which there is not a priori knowledge of the magnitude and direction of the source polarization.

Data were also obtained on the magnitude of long time-constant effects in the MIRS detectors. Previous experience with bulk-doped silicon photoconductors indicated that time-

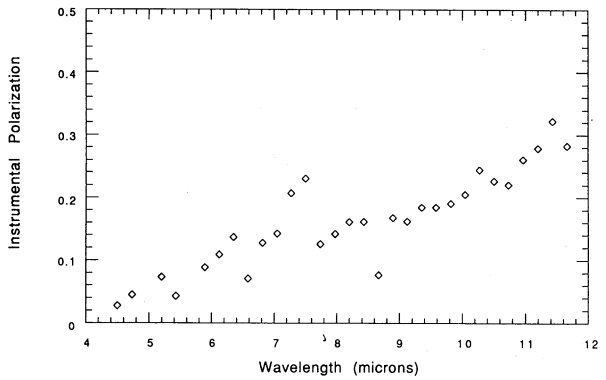

FIG. 4.—Instrumental polarization in the MIRS. The instrumental polarization is defined as the fraction of linearly polarized light lost in transmission through the instrument when the incident beam position angle is orthogonal to the instrumental polarization direction.

dependent variations in the detector responsivity are common in low-infrared background environments (Beichman et al. 1988). The magnitude of such variations in the MIRS detectors was measured by applying a variable-length step function to the infrared flux received by the MIRS. Although some of the MIRS detectors exhibited responsivity changes lasting up to 4 minutes in length, the magnitude of these changes was never greater than 8% in the worst cases. These responsivity changes were also observed to increase in magnitude with increases in the infrared flux received, so the realistic responsivity variations are expected to be less than 3% for all except the few very brightest sources seen by the MIRS while on-orbit. Previous laboratory investigations with similar Si:Bi detectors have indicated that any on-orbit ionizing radiation-induced responsivity changes are expected to be less than 5%.

Measurements were also taken at different MIRS operating temperatures to determine the instrument sensitivity to variations in the IRTS cryostat temperature. The instrument signal response was found to decrease by a factor of 2 when the temperature was reduced from 4.2 to 2.0 K. However, the temperature response curve was fairly flat for temperatures near the expected operating temperature; the instrument responsivity changed by only 0.9% when the temperature was increased from 1.75 to 2.17 K.

5. THE MIRS INSTRUMENTAL SENSITIVITY

Based on the signal and noise data from these laboratory tests, the MIRS on-orbit surface-brightness sensitivity was derived and is shown in Figure 5 in a λF_λ plot. In this plot, the estimated MIRS 1 σ sensitivity for one MIRS beam size is indicated by the filled black diamonds, assuming that the IRTS great circle scans are offset from one another by one-half of an MIRS beam size. This estimate includes the contributions from both the measured instrumental noise as well as the estimated Zodiacal background noise. The fine line associated with the diamonds is the sensitivity limit arising from fluctuations in the Zodiacal background alone. As can be seen, the MIRS is Zodiacal background-limited in sensitivity at all but the shortest wavelengths. The derived MIRS sensitivity given above is likely to be affected by systematic errors from a number of sources in our laboratory measurements, including uncertainties in the transmission of the test cryostat optical train, less-than-ideal performance of the blackbody sources, and particularly by the fact that the MIRS grating was only being partially illuminated in our laboratory test setup. Making our best estimates of the worst-case magnitudes for these systematic error sources, we find that the MIRS sensitivity line in Figure 5 could possibly be moved up or down by as much as the amount indicated by the barred symbol in the figure. As with the spectral resolution, the true instrumental sensitivity will have to be determined by observations of standard sources while on-orbit.

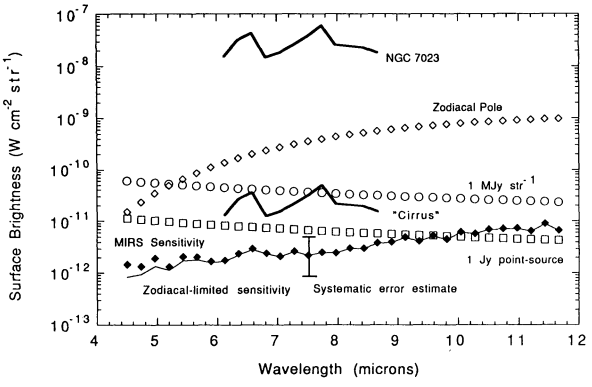

FIG. 5.—Sensitivity of the MIRS in a λF_λ plot, expressed as a 1 σ surface-brightness limit. The total predicted sensitivity of the MIRS is shown by the filled diamonds. The sensitivity limits imposed by fluctuations in the Zodiacal background are shown by the fine line associated with the filled diamonds. The worst-case estimate of the effects of systematic errors in the laboratory calibration are shown by the barred symbol. For comparison, the surface brightness of various infrared sources is also indicated and are explained in more detail in the text.

The three primary science goals of the MIRS are to (*a*) take spectra of the diffuse Galactic emission (cirrus), (*b*) take spectra of the Zodiacal light, and (*c*) measure the spectra of the estimated 9800 point sources that will fall within the IRTS scan path and are bright enough to be seen by the MIRS. The ability of the MIRS to meet these science goals is also shown in Figure 5. In this figure, the observed spectrum of the extended reflection nebula NGC 7023 from Sellgren et al. (1985) is shown. A second spectrum of NGC 7023 is also displayed, but in this case shifted down in flux in order to match the intensity of a typical Galactic infrared cirrus cloud observed by *IRAS* (Boulanger et al. 1985). If this shifted spectrum can be used as an estimate of what may be expected from an average cirrus cloud, it can be seen that MIRS will have enough sensitivity to measure the spectral features at a signal-to-noise of over 5:1, even with the worst-case estimate of the instrument sensitivity. If the "generic" IR emission feature strength ratios from Cohen et al. (1986) are used to extrapolate the strength of the 7.7 μm feature from the measured emission from the 3.3 μm feature (Giard et al. 1989), it can be seen that the diffuse emission from the 7.7 μm feature should be detected by the MIRS to Galactic latitudes greater than $|b| > 10°$.

The flux from the Zodiacal pole is shown in Figure 5 as open diamonds. It can be seen that the MIRS has the sensitivity to measure the spectrum of this emission at very high signal-to-noise. The observed flux from a hypothetical 1 Jy point-source is shown as open squares, as is the observed flux from a hypothetical 1 MJy-steradian^{-1} extended source, shown as open circles. The high point-source sensitivity of the MIRS will ensure that most of the *IRAS* 12 μm point sources will also be bright enough for MIRS spectral studies. Confusion from more than one point source within the MIRS beam may turn out to be the limiting factor in the ability of the MIRS to detect faint point sources at some wavelengths. For the longest MIRS wavelengths, the *IRAS* data set gives an estimate of approximately 34 sources per square degree that will be seen by the MIRS at the 1 σ level in the center of the Galactic plane ($|b| < 0.°05$, averaged over all Galactic longitudes; Cohen et al. 1990). As the MIRS beam is only $0.°14 \times 0.°14$ in size, the average number of *IRAS* 12 μm point sources in the MIRS beam within the plane is 0.67. As a result, at the longer MIRS wavelengths point-source confusion is only just starting to become a problem. At the short end of the MIRS wavelength range, the situation is likely to be worse. At 4.8 μm the MIRS 1 sigma point-source sensitivity is approximately 0.2 Jy or +7.2 magnitude. Estimating the density of sources at this wavelength is difficult, but an upper limit can be approximated by using the density of 2.2 μm sources from the sky model of Cohen et al. (1990). Using this model in the Galactic plane ($l = 49.°7$, $b = 0.°16$) we find a number density of approximately

100 sources per square degree brighter than +7.2 mag at K (2.2 μm). For the MIRS beam this translates into an average of 2 sources per beam in the Galactic plane. It is therefore likely that the MIRS will be confusion-limited at its shortest wavelengths within the center of the Galactic plane.

6. CONCLUSIONS

A Mid-Infrared Spectrometer (MIRS) for the Infrared Telescope in Space mission has been constructed, tested, and calibrated in the laboratory. The MIRS has met all of the design objectives and will able to make a very high sensitivity survey of up to 10% of the sky, including both point-sources and extended objects. This high sensitivity will allow spectral studies of low surface-brightness extended objects, the Zodiacal dust emission, and many of the point-sources in the *IRAS* survey.

We are grateful for the support of this program from the NASA Astrophysics Grants Program and the Institute for Space and Astronomical Science. We also wish to thank the many people who contributed to the construction of this instrument, including N. Jennerjohn, M. Brousse, R. Zieger, and D. Lesberg. We would also like thank S. Sandford and other members of the NASA/Ames Astrophysics Laboratory for their assistance in measuring some of the MIRS filter transmission curves. Finally, we wish to thank A. Sakata, H. Okuda, T. Matsumoto, H. Shibai, H. Murakami, and M. W. Werner for useful discussions and help on this project.

REFERENCES

Beichman, C. A., Neugebauer, G., Habing, H. J., Clegg, P. E., & Chester, T. J. 1988, Infrared Astronomical Satellite (*IRAS*), Catalogs and Atlases, Vol. 1 (NASA RP 1190)
Bock, J. Matsuhara, T. Matsumoto, T., Onaka, T., Sato, S., & Lange, A. E. 1993, Appl. Opt., submitted
Boulanger, F., Baud, B., & van Albada, G. D. 1985, A&A, 144, L9
Cohen, M., Allamandola, L., Tielens, A. G. G. M., Bregman, J., Simpson, J. P., Witteborn, F. C., Wooden, D., & Rank, D. 1986, ApJ, 302, 737
Cohen, M., Walker, R., Wainscoat, R., Volk, K., Walker, H., & Schwartz, D. 1990, An Infrared Sky Model Based on the *IRAS* Point Source Data (NASA Contractor Rep. 177526).
Giard, M., Pajot, F., Lamarre, J. M., Serra, G., & Caux, E. 1989, A&A, 215, 92
Harada, T., & Kita, T. 1980, Appl. Opt., 19, 3987
Lange, A. E., Freud, M., Sato, S., Hirao, T., Matsumoto, T., & Watabe, T. 1994, ApJ, 428, 384
Murakami, H., et al. 1994, ApJ, 428, 354
Noda, M., Christov, V. V., Matsuhara, S. Noguchi, K., Sato, S., & Murakami, H. 1994, ApJ, 428, 363
Onaka, T. 1994, in preparation
Onaka, T., et al. 1993, Appl. Opt., in press
Sellgren, K., Allamandola, L. J., Bregman, J. D., Werner, M. W., & Wooden, D. H. 1985, ApJ, 299, 416
Shibai, H., Yui, M., Matsuhara, H., Hiromoto, N., Nakagawa, H., & Okuda, H. 1994, ApJ, 428, 377
Young, E. 1989, private communication